# FINAL REPORT (1999–2001)

GLOBAL AEROSOL CLIMATOLOGY PROJECT:
Improvement and Synthesis of Global Aerosol Climatologies
Derived from Long-Term Satellite Observations and
3D Transport Models

Michael I. Mishchenko (GISS), PI
Andrew A. Lacis (GISS), CoI
Igor V. Geogdzhayev (CU), CoI
Ina Tegen (CU), CoI
Brian Cairns (CU), CoI
Jacek Chowdhary (CU), CoI

## 1. AVHRR Data Analyses

Since the operational AVHRR algorithm (Stowe et al., 1997) utilizes only one datum per pixel (channel 1 reflectance at a single observation geometry), it can retrieve only one model parameter (optical thickness), whereas all remaining parameters must be fixed *a priori*. It has been suggested that the use of channel 2 as well as channel 1 reflectance measurements can provide additional information on the aerosol model and also improve the accuracy of the optical thickness retrieval (Durkee et al., 1991; Nakajima and Higurashi, 1998). The papers by Mishchenko et al. (1999) and Geogdzhayev et al. (2002) outlined the methodology of inverting channel 1 and 2 AVHRR radiance data over the oceans, described a detailed analysis of the sensitivity of monthly averages of retrieved aerosol parameters to the assumptions made in different retrieval algorithms, and presented a preliminary global aerosol climatology for the period of NOAA-7, -9, and -11 observations. The sensitivity analysis was based on using real AVHRR data and exploiting accurate numerical techniques for computing single and multiple scattering and spectral absorption of light in the vertically inhomogeneous atmosphere-ocean system. It was assumed initially that aerosol particles were homogeneous spheres so that their scattering and absorption properties could be computed using the standard Lorenz-Mie theory. Theoretical channel 1 and 2 reflectances were calculated using a radiative transfer code based on the scalar version of the adding/doubling method. The numerical procedure incorporated the rough ocean surface reflection via the modified Kirchhoff approximation, the water vapor, oxygen, and $CO_2$ absorption via the k-distribution technique, and gaseous scattering. The upwelling radiances from the ocean body and foam scattering were either ignored or modeled by adding a small Lambertian component to the surface bidirectional reflection function. The atmospheric temperature and humidity profiles were taken from the ISCCP version of the TOVS data, while the vertical distribution of ozone and water vapor was based on a standard atmospheric profile. The vertical profile of aerosol was taken to be the same as the normalized profile of water vapor. The radiative transfer code was

used to compute a look-up table in which multidimensional arrays of theoretical channel 1 and 2 reflectance values for all viewing geometries and aerosol and atmospheric parameters were stored. The look-up table was then used to retrieve the aerosol optical thickness and size using cloud-screened channel 1 and 2 radiance data. Each pixel was mapped on a 1° by 1° global grid. The retrieved values of the aerosol parameters for all pixels within one grid cell were averaged to produce a map for a specified period of time.

The main results of this sensitivity study of the expected performance of two-channel aerosol retrieval algorithms can be summarized as follows.

- Two-channel algorithms can be expected to provide significantly more accurate and less biased retrievals of the aerosol optical thickness than one-channel algorithms.

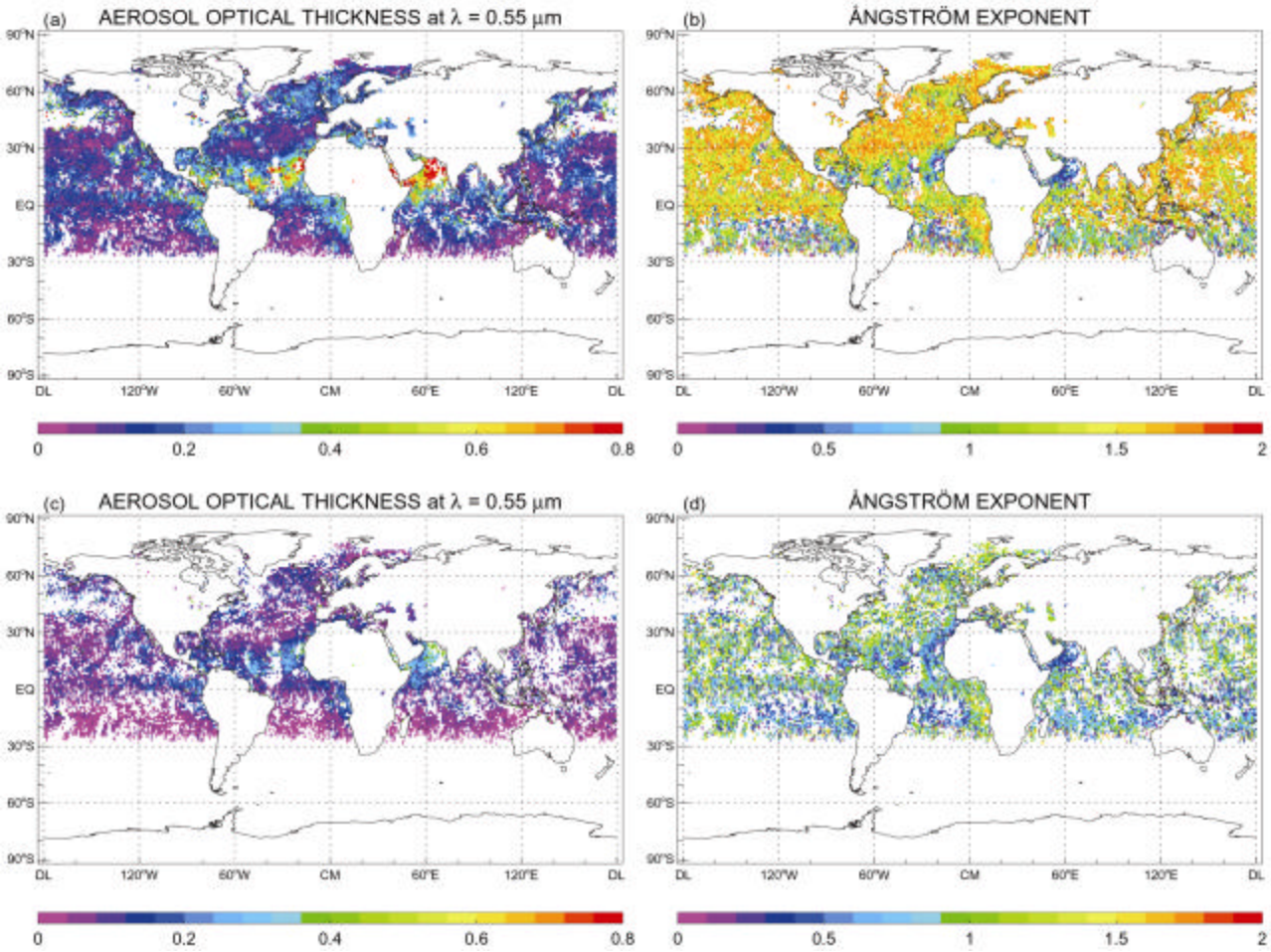


Fig. 1. Monthly mean aerosol optical thickness and Ångström exponent for July 1988. (a) and (b): The average t and A values are computed using all clod-free pixels. (c) and (d): The average t and A values are computed using only pixels with $0 < A < 1.75$.

- Imperfect cloud screening is a major source of errors in the retrieved optical thickness. This problem is difficult to solve definitively and should be addressed by means of extensive ground-based observations, careful statistical analyses of the radiance data, and, potentially, comparisons with future results from more advanced satellite instruments.
- Two different ways of computing the average aerosol size (direct versus optical-thickness-weighted) can be expected to produce similar results because of weak correlation between the aerosol optical thickness and size.
- Both underestimating and overestimating aerosol absorption as well as the potentially strong variability of the real part of the aerosol refractive index may lead to regional and/or seasonal biases in the retrieved aerosol optical thickness.

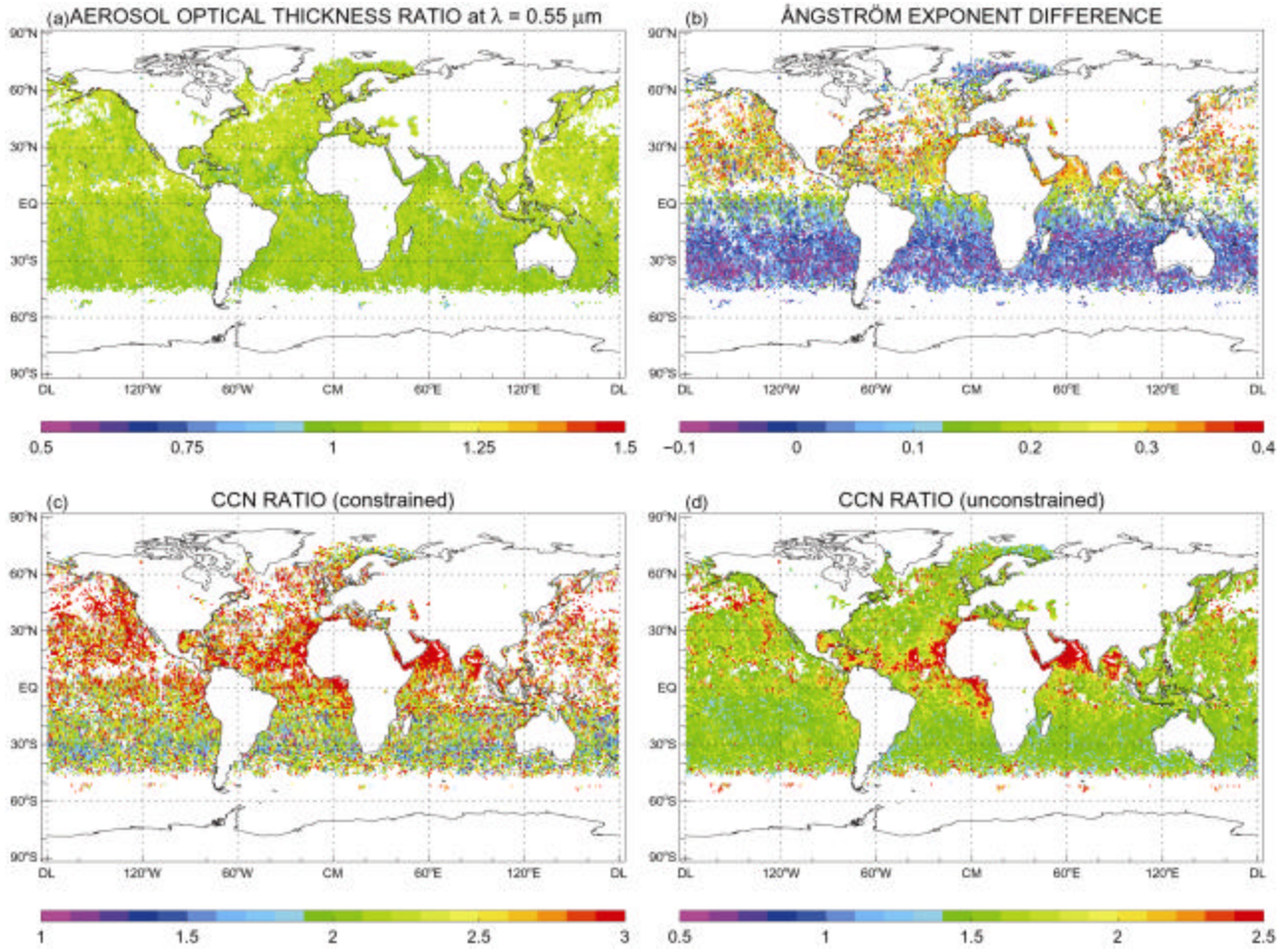


Fig. 2. (a): Ratio of monthly mean aerosol optical thicknesses retrieved with the bimodal size distribution and the power law distribution. (b): As in (a), but for the difference of constrained monthly mean Ångström exponents. (c): As in (a), but for the CCN column number density retrieved with constrained Ångström exponents.

(d): As in (a), but for the CCN column number density retrieved with unconstrained Ångström exponents.

- Neglecting the diffuse component of the ocean reflection function can affect the retrieved optical thickness in the cases of low aerosol loads.
- Simple monthly average of the Ångström exponent appears to be the most invariant aerosol size characteristic and should be retrieved along with optical thickness as the second aerosol parameter.
- For some pixels the best retrieval in terms of yielding the minimal difference between the measured and modeled radiances is obtained for Ångström exponents corresponding to either the maximal (1.75) or the minimal (0.0) A value allowed by our look-up tables. The effect is clearly discernable in the maps of the monthly mean Ångström exponent (Fig. 1). This creates a problem of how the pixels yielding either A = 0 or A = 1.75 should be treated. For example, very small retrieved Ångström exponents correspond to large particles and may be interpreted as a sign of undetected cloud contamination. Alternatively, the cases of out-of-range Ångström exponent values may be caused by imperfect radiance calibration or result from using fixed global values of certain model parameters that are significantly different from their actual values for specific pixels at the time of the measurement. Given this uncertainty, it has been decided to modify the final aerosol product by creating two separate Ångström exponent data sets which may be called “constrained” and “unconstrained” versions. In the unconstrained version, all pixels are taken into account in computing the average A value, whereas the constrained version excludes pixels with A = 0 or A = 1.75. In both cases all pixels contribute to the optical thickness average.
- Radiance calibration uncertainties may be among the main factors hampering the retrieval accuracy. Specifically, the addition/subtraction of one digital count to/from the AVHRR radiances can cause changes in the retrieved aerosol optical thickness exceeding 40% in open ocean areas. Given the significant spread in the published calibration constants, it is unlikely that a significant breakthrough in the retrieval accuracy may be achieved based on the AVHRR data alone. Instead, the way to solve the calibration problem may be to use advanced global satellite retrievals (Kahn et al. 1998, 2001; Tanré et al. 1997; Deuzé et al. 2000) as a benchmark.
- The two-channel algorithm shows a significant degree of insensitivity to a specific choice of the aerosol particle size distribution function. One should expect only small (. 10%) changes in the retrieved aerosol optical thickness and changes less than 0.3 in the Ångström exponent when switching from one size distribution function to another [Figs. 2(a) and 2(b)]. This conclusion appears to be independent of other model and calibration assumptions.

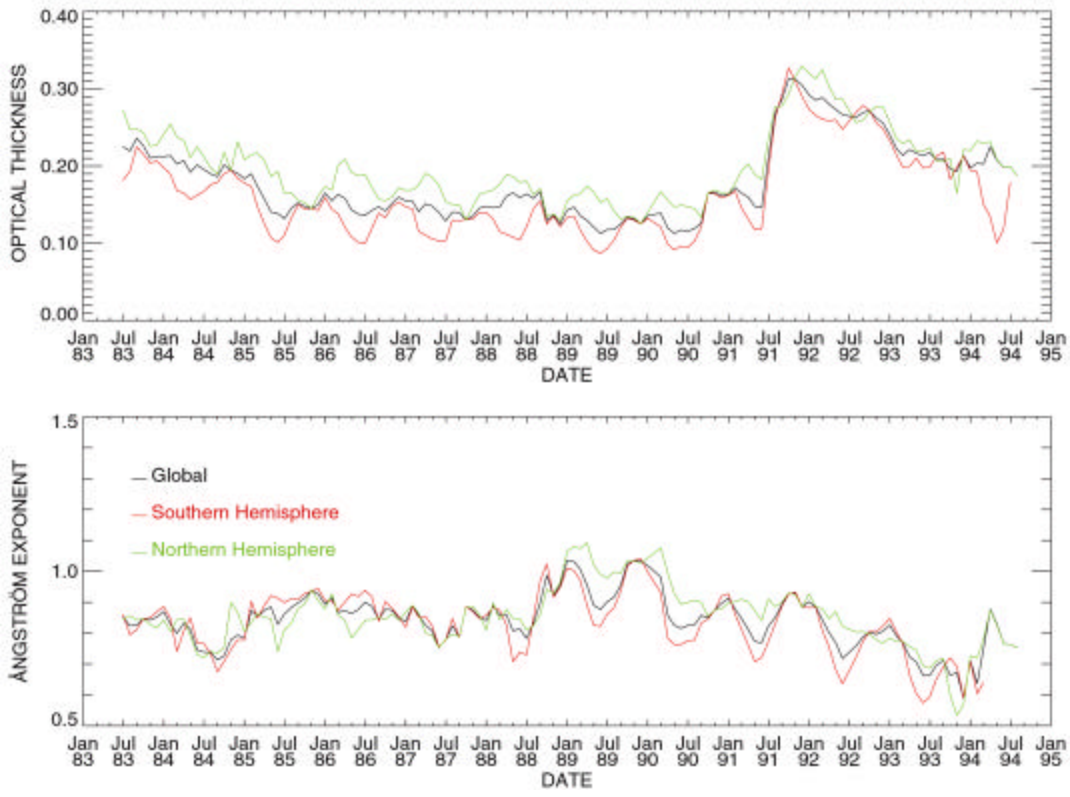


Fig. 3. Global and hemispherical monthly averages of the aerosol optical thickness and constrained Angström exponent for the period of July 1983–August 1994.

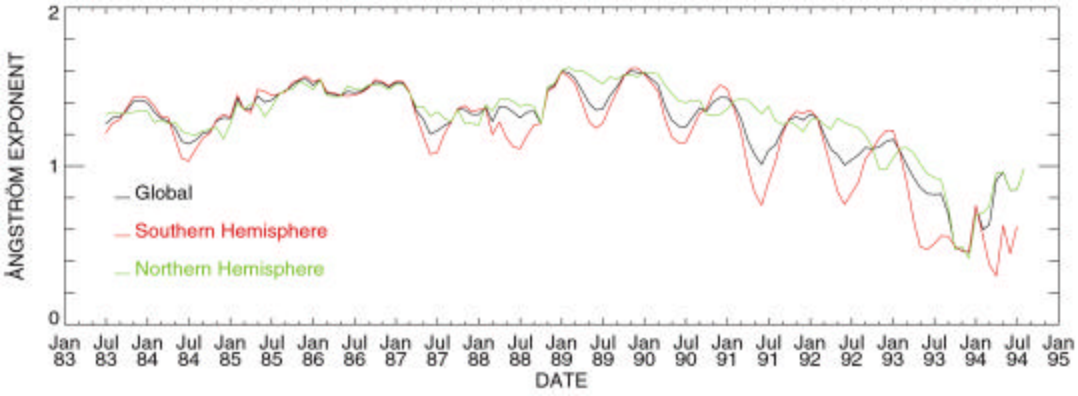


Fig. 4. Global and hemispherical monthly averages of the unconstrained Ångström exponent for the period of Jul 1983–Aug 1994.

- The CCN column number density cannot be reliably retrieved from the two-channel AVHRR data. A change in the assumed analytical representation of the aerosol particle size distribution can lead to changes in the retrieved CCN concentration exceeding 300% [Figs. 2(c) and 2(d)].

- The assumption of a fixed global value of the wind speed leads to errors less than 10% in the retrieved aerosol optical thickness and less than 0.125 in the Ångström exponent relative to the results obtained using real-time wind speed data. Taking real-time wind speed data into account may improve the accuracy of regional retrievals in the areas where strong wind patterns exist, although on the global scale the accuracy gain may be masked by other uncertainties.
- Global monthly mean values of the aerosol optical thickness show no significant trend over the lifetime of the NOAA-9 satellite (February 1985 through November 1988), Figs. 3 and 4. The derived average global values are 0.15 for the optical thickness and 0.85 for the constrained Ångström exponent. However, these values depend on the assumed calibration and aerosol optical model, the main source of errors being the uncertainty in the deep space count.
- There is a discontinuity in the retrieved Ångström exponents at the time of NOAA-9 to NOAA-11 transition and a significant trend in the Ångström exponent not consistent with the Mt. Pinatubo eruption (Figs. 3 and 4). This is likely to be an indication of a serious calibration problem.
- The NOAA-9 record reveals a seasonal cycle with maxima occurring around January-February and minima in June-July in the globally averaged aerosol optical thickness. The Northern hemisphere mean optical thickness systematically exceeds that averaged over the Southern hemisphere. Zonal means of the optical thickness exhibit an increase in the tropical regions of the Northern hemisphere associated with annual desert dust outbursts and a spring time increase at middle latitudes of the Northern hemisphere. Increased aerosol loads observed at middle latitudes of the Southern hemisphere are probably associated with higher sea salt particle concentrations. Reliable extension of the retrieval record beyond the NOAA-9 lifetime will help to corroborate these findings.

Although the initial processing of the entire ISCCP data set is essentially completed, several important issues still need to be addressed. These include an improved calibration of AVHRR channel 1 and 2 radiances, the inclusion of stratospheric aerosols for the periods of volcano eruptions, and the effect of nonsphericity of dust-like aerosols on the optical thickness and Angstrom exponent retrievals. The expected final result will be a flexible and compact algorithm that could be combined with the ISCCP cloud retrieval algorithm and used for simultaneous operational retrievals of cloud and aerosol properties. Further research will focus on validation and fine-tuning of the aerosol algorithm based on various kinds of in situ, ground-based, and aircraft data and calibration of the global aerosol product using more advanced results from the MODIS and MISR instruments.

## 2. Polarization and Depolarization Data Analyses

Chowdhary et al. (2001, 2002) performed a detailed analysis of high-precision radiance and polarization data obtained over the ocean by an airborne version of the Earth Observing Scanning Photopolarimeter (EOSP), the research Scanning Polarimeter (RSP). The analysis has shown that bimodal size information, composition (via refractive index), aerosol optical depth and number density can be retrieved from multi-spectral, multiangle polarization measurements. The aerosol optical depth retrieved from the RSP data is consistent with sun-photometer measurements (differences less than 0.01 at 0.55 μm). The weak sensitivity of polarized reflectances at shorter wavelengths (0.41 and 0.55 μm) to ocean color allows for their inclusion in the retrieval of aerosol properties and shows the potential of polarimetry to separate ocean color monitoring from atmospheric correction. It has been demonstrated that analyses of reflectance-only data subsets are not capable of distinguishing monomodal from bimodal aerosol solutions, nor do they provide strong constraints on aerosol refractive indices. The errors in aerosol retrievals from these reflectance-only data subsets are seen to propagate into errors in the estimated ocean color. The simulated examples of POLDER retrievals indicates useful sensitivity to the refractive index, size and optical depth of the accumulation mode aerosol, but the absence of longer wavelength (2.25 μm) measurements limits the amount of information that can be obtained about the coarse mode aerosol. Since the errors in the estimated accumulation mode are small the estimate of ocean color from the POLDER-like data subset is similar to that obtained from the complete data set, suggesting that the inclusion of polarized reflectances from the shorter wavelength bands of POLDER may be useful in improving aerosol retrievals from this type of data.

The accurate polarimetric measurements made by the RSP, over a broad angular and spectral range, significantly reduce the non-uniqueness problem in the retrieval of aerosol properties by providing information about the spectral refractive index and both accumulation and coarse mode size distribution parameters. This capability allows aerosol parameters to be determined with the accuracy needed for long-term monitoring of the direct and indirect aerosol forcings of climate. The analysis of polarized reflectances at shorter wavelengths (0.41 and 0.55 μm) indicates the potential of these measurements to further improve aerosol retrievals and atmospheric correction for ocean color monitoring.

Although polar stratospheric clouds (PSCs) are unlikely to cause a significant direct radiative forcing of climate, their critical role in chemical ozone depletion is now well recognized (e.g., Carslaw et al., 1998, and references therein). The traditional classification of PSC types is based on lidar observations (Browell et al. 1990). Type Ia PSCs are characterized by low backscattering but strong depolarization, whereas type Ib PSCs exhibit the opposite behavior. Type II PSCs demonstrate both strong backscatter and large depolarization ratios. Type Ib clouds are believed to consist of droplets of supercooled ternary solutions (STSs) of water, nitric acid, and sulfuric acid, whereas type Ia PSCs are thought to form by condensation of nitric acid tri- or dihydrate (NAT or NAD). Type II PSCs are thought to consist of water ice crystals. Based on extensive *T*-matrix computations of light scattering by polydispersions of randomly oriented, rotationally

symmetric nonspherical particles, Liu and Mishchenko (2001) have analyzed existing lidar observations of PSCs and derived several constraints on PSC particle miscrophysical properties. They have shown that sharp-edged nonspherical particles (finite circular cylinders) exhibit less variability of lidar backscattering characteristics with particle size and aspect ratio than particles with smooth surfaces (spheroids). For PSC particles significantly smaller than the wavelength, the backscatter color index $\alpha$ and the depolarization color index $\beta$ are essentially shape-independent. Observations for type Ia PSCs can be reproduced by spheroids with aspect ratios larger than 1.2, oblate cylinders with diameter-to-length ratios greater than 1.6, and prolate cylinders with length-to-diameter ratios greater than 1.4. The effective equal-volume-sphere radius for type Ia PSCs is about $0.8\,\mu\mathrm{m}$ or larger. Type Ib PSCs are likely to be composed of spheres or nearly spherical particles with effective radii smaller than 0.8 μm. Observations for type II PSCs are consistent with large ice crystals (effective radius greater than 1 μm) modeled as cylinders or prolate spheroids.

## 3. The effect of black carbon aerosols on scattering and absorption of solar radiation by cloud droplets

Black carbon (BC) has long been recognized as an important atmospheric pollutant (Penner and Novakov, 1996). It plays a significant role in the absorption of solar radiation by atmospheric aerosols and possibly also by clouds. Enhanced absorption by black carbon particles imbedded in water droplets could potentially reduce the cloud albedo (Chýlek et al., 1984), thereby causing a significant indirect forcing of climate (Charlson et al., 1992). Liu et al. (2002) have calculated scattering and absorption characteristics of water cloud droplets containing black carbon (BC) inclusions at a visible wavelength of 0.55 μm using a combination of ray-tracing and Monte Carlo techniques. In addition, Lorenz-Mie calculations have been performed assuming that the same amount of BC particles are mixed with water droplets externally. The results show that it is unlikely under normal conditions that BC aerosols can modify scattering and absorption properties of cloud droplets in any significant way except for geographical locations very close to major sources of BC. The differences in the single-scattering co-albedo and asymmetry parameter between BC-fraction-equivalent internal and external mixtures are negligibly small for normal black carbon loadings. For a fixed amount of BC internally mixed with cloud droplets, the absorption is maximal when the effective radius of the BC inclusions is about 0.05–0.06 μm.

## 4. Aerosol Transport Modeling

Current retrievals of aerosol optical properties from satellites lack global coverage and are especially difficult over land. Therefore, results from 3-dimensional aerosol chemistry/transport models can be useful to fill in coverage gaps. These models compute aerosol distributions from source emissions using prescribed meteorological fields to calculate aerosol transport, mixing, transformation, and deposition. Such calculations can

be carried out for each of the important aerosol types individually. Ground-based measurements and satellite-derived aerosol distributions are used to validate and constrain these models. On the other hand, the results from transport models can be used as 'first guess' scenarios in satellite retrievals. In this way both satellite retrievals and model transport calculations of distributions of aerosol properties can be improved iteratively. When better satellite instruments, retrieval algorithms, and models become available, the combined aerosol product will become increasingly accurate.

As a first step, Tegen et al. (URL: http://gacp.giss.nasa.gov/transport) provided model-derived distributions of aerosol optical thickness. Resulting distributions for the main aerosol species (sulfate, soil dust, carbonaceous aerosols and sea salt) from different transport models by several authors were combined to estimate the individual contributions to the total aerosol optical thickness. The aerosol transport models, from which the results were derived, were developed by Chin et al. (1996) for sulfates; Tegen and Fung (1995) for soil dust; Tegen et al (1997) for sea salt; and Liousse et al. (1996) for carbonaceous aerosols and black carbon.

## 5. Peer-Reviewed Publications


Cairns, B., M. Mishchenko, L. Travis, and J. Chowdhary (2001). Reply to comment on "Retrieval of aerosol properties over the ocean using multispectral and multiangle photopolarimetric measurements from the Research Scanning Polarimeter," *Geophys. Res. Lett.* **28**, 3277–3278.

Chowdhary, J., B. Cairns, M. Mishchenko, and L. Travis (2001). Retrieval of aerosol properties over the ocean using multispectral and multiangle photopolarimetric measurements from the Research Scanning Polarimeter, *Geophys. Res. Lett.* **28**, 243–246.

Geogdzhayev, I. V., and M. I. Mishchenko (1999). Sensitivity analysis of aerosol retrieval algorithms using two-channel satellite radiance data, *Proc. SPIE* **3763**, 155–168.

Geogdzhayev, I. V., and M. I. Mishchenko (2001). Expanding GACP aerosol climatology beyond NOAA-9 AVHRR lifetime. *Proc. SPIE* **4539**, in press.

Geogdzhayev, I. V., M. I. Mishchenko, W. B. Rossow, B. Cairns, and A. A. Lacis (2002). Global two-channel AVHRR retrievals of aerosol properties over the ocean for the period of NOAA-9 observations and preliminary retrievals using NOAA-7 and NOAA-11 data, *J. Atmos. Sci.*, in press.

Haywood, J. M., P. N. Francis, I. Geogdzhayev, M. Mishchenko, and R. Frey (2001). Comparison of Saharan dust aerosol optical depth retrieved using aircraft mounted pyranometers and 2-channel AVHRR algorithms, *Geophys. Res. Lett.*, **28**, 2393–2396.

Liu, L., and M. I. Mishchenko (2001). Constraints on PSC particle microphysics derived from lidar observations, *J. Quant. Spectrosc. Radiat. Transfer* **70**, 817–831.

Liu, L., M. I. Mishchenko, S. Menon, A. Macke, and A. A. Lacis (2002). The effect of black carbon on scattering and absorption of solar radiation by cloud droplets, *J. Quant. Spectrosc. Radiat. Transfer* (submitted).

Mishchenko, M. I. (2000). Calculation of the amplitude matrix for a nonspherical particle in a fixed orientation, *Appl. Opt.* **39**, 1026–1031.

Mishchenko, M. I., and A. A. Lacis (2000). Manifestations of morphology-dependent resonances in Mie scattering matrices, *Appl. Math. Comput.* **116**, 167–179.

Mishchenko, M. I., and L. D. Travis (2000). Polarization and depolarization of light. In *Light Scattering from Microstructures* (F. Moreno and F. Gonzalez, Eds.), Springer-Verlag, Berlin, pp. 159–175.

Mishchenko, M. I., and L. D. Travis (2002). Electromagnetic scattering by nonspherical particles. In *Exploring the Atmosphere by Remote Sensing* (R. Guzzi and K. Pfeilsticker, Eds.), Springer-Verlag, Heidelberg, pp. 1–46 (in press).

Mishchenko, M. I., I. V. Geogdzhayev, B. Cairns, W. B. Rossow, and A. A. Lacis (1999). Aerosol retrievals over the ocean by use of channels 1 and 2 AVHRR data: sensitivity analysis and preliminary results, *Appl. Opt.* **38**, 325–7341.

Mishchenko, M., J. Penner, and D. Anderson (2002). Editorial: Global Aerosol Climatology Project, *J. Atmos. Sci.*, in press.

Penner J. E., S. Y. Zhang, M. Chin, C. C. Chuang, J. Feichter, Y. Feng, I. V. Geogdzhayev, P. Ginoux, M. Herzog, A. Higurashi, D. Koch, C. Land, U. Lohmann, M. Mishchenko, T. Nakajima, G. Pitari, B. Soden, I. Tegen, and L. Stowe (2002). A comparison of model- and satellite-derived aerosol optical depth and reflectivity, *J. Atmos. Sci.*, in print.

Yang, P., K. N. Liou, M. I. Mishchenko, and B.-C. Gao (2000). Efficient finite-difference time-domain scheme for light scattering by dielectric particles: application to aerosols, *Appl. Opt.* **39**, 3727–3737.